DOI: https://doi.org/10.31351/vol35iss2pp50-65

Tizanidine Cubosomal Nano Carriers as Transdermal Delivery System: Preparation and Characterization

Milad Jawad Hasan*,[1] and Nawal Ayash Rajab[2]

[1]Ministry of Health, National Center for Drugs Control &Research, Baghdad, Iraq.

[2]Department of Pharmaceutics, College of Pharmacy, University of Baghdad, Baghdad, Iraq.

***Corresponding author**

Received 28/2/2025, Accepted 13/7/2025, Published 24/6/2026

Abstract

Cubosomes are nanoscale lipidic dispersions in an aqueous medium, formed through a spontaneous and highly ordered self-assembly mechanism. These lipid-based dosage forms can serve as effective carriers for both lipophilic and hydrophilic drugs, thereby enhancing their therapeutic efficacy. In this study, cubosomes were developed to investigate their potential as nanocarriers for the transdermal delivery of tizanidine, a centrally acting skeletal muscle relaxant with low oral bioavailability. The cubosomal vesicles were prepared using the thin-film hydration technique, where glyceryl monooleate constituted the lipid matrix, and poloxamer 407 functioned as the stabilizing agent. To optimize the formulation, a Central Composite Design was applied using Design-Expert® software version 13, The impact of the selected concentrations of GMO and P407, considered as independent variables, was assessed on particle size, polydispersity index, and entrapment efficiency (%EE). Vesicle characteristics were modified by varying the surfactant-to-lipid ratio.

The prepared formulations were evaluated for vesicle size, polydispersity index, and drug entrapment efficiency. The formulation exhibiting optimal characteristics was subsequently assessed for in vitro drug release behavior and zeta potential, field emission scanning electron microscopy, and compatibility studies using Fourier-transform infrared spectroscopy. Additionally, differential scanning calorimetry was performed to compare the optimized formulation with the pure drug. The results demonstrated significant variations in physicochemical properties such as particle size and entrapment efficiency.

The optimized formulation, designated as F9, exhibited a vesicle size of 160.7 ± 4.79 nm, a polydispersity index of 0.061 ± 0.048, an entrapment efficiency of 76.8 ± 0.17%, and a zeta potential of –23.46 ± 4.09 mV. Results from the in vitro release study confirmed a consistent and sustained drug release profile from the cubosomal dispersion. Photomicrographic analysis confirmed a uniform cubic morphology with good dispersion stability. These findings indicate that the thin-film hydration technique is a promising method for developing stable and effective cubosomal drug delivery systems.

Keywords: cubosomes, muscular spasm, tizanidine , transdermal delivery, vesicular System.

Introduction

As an innovative drug delivery mechanism, cubosomes the cubic phase of liquid crystalline nanoparticles is gaining a lot of interest (Figure 1). They are made up of a bicontinuous structure consisting of two non-intersecting water channels divided by a highly twisted continuous lipid bilayer [1,2]. Cubosomes are often made by allowing amphiphilic lipids, including phytantriol and glycerol monooleate (GMO), to self-assemble while stabilizing the process with poloxamer 407[3–5]. The majority of the lipids in the formulation are thermally stable, biocompatible, non-allergic, non-irritating, and nontoxic [6]. Cubosomes' distinct shape allows for the incorporation of both hydrophilic and hydrophobic drugs, including proteins, peptides, amino acids, and nucleic acids as well as small-molecular weight drugs [7–9] it is possible to encapsulate hydrophilic drugs in water channels and hydrophobic drugs in the structure's lipid bilayers [10–12]. Furthermore, for a variety of drugs, cubosomes provide targeted and controlled release characteristics [13,14]. Due to their above-mentioned promising qualities, cubosomes are frequently employed for drug administration via intravenous, oral, percutaneous, and ocular routes [15–18]. While cubosomes are often used for lipophilic and poorly water-soluble drugs, their internal structure also allows encapsulation of hydrophilic and amphiphilic drugs. Moreover, their ability to provide controlled and sustained release makes them ideal for drugs with limited bioavailability, protection from enzymatic degradation , and the

potential to enhance transdermal and systemic delivery of drugs with challenging pharmacokinetic profiles. Drugs that exhibit poor oral bioavailability, extensive first-pass metabolism, or require prolonged systemic effect are ideal candidates.

Spasticity is a frequent symptom associated with neurologic illnesses that can cause discomfort from contracting muscles and impair movement. When a muscle is passively extended, it results in a continuous rise in tone [19,20], from little muscular stiffness to severe, painful, and uncontrolled muscle spasms, it can fluctuate in severity. It is linked to a number of prevalent neurological conditions, including spinal cord and brain traumas, cerebral palsy, multiple sclerosis, stroke, and neurodegenerative illnesses impacting the pyramidal and extrapyramidal pathways, as well as higher motor neurons [21]. Oral medications are recommended when spasticity symptoms interfere with a patient's regular way of life. The most commonly recommended medications include skeletal muscle relaxants such as baclofen, tizanidine, imidazoline derivatives, gabapentin, and dantrolene [22].

Tizanidine (TZN) has several notable benefits, including greater selectivity, reduced risk of hypotension and weakness [23]. Tizanidine is a centrally-acting muscle relaxant. this medicine is a myotonolytic agent that functions as a central alpha-2 adrenoceptor agonist. it is used for the treatment of spasms in individuals who have experienced brain or spinal injury [24]. Tizanidine has a half-life of 2.5 hours and is eliminated from the body through the kidneys 60% and the feces 20% [25]. Figure 2 illustrates the molecular structure of tizanidine.

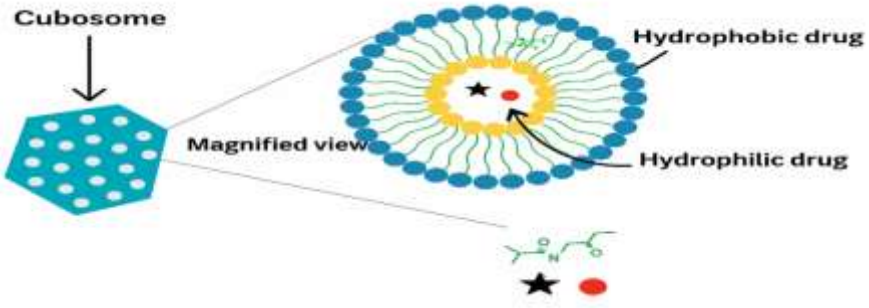

Figure 1. Structural illustration of a lipid cubosome vesicular system [5]

Tizanidine has limited oral bioavailability as a result of substantial first-pass metabolism. Its short half-life necessitates frequent dosing to maintain therapeutic plasma concentrations. The dosage of the medication can be escalated to 36 mg, depending on the duration and intensity of the illness. typically, a regimen of 2 to 4 mg administered three to four times daily [26]. Multiple research papers exist that discuss formulations aimed at improving the bioavailability and reducing the frequency of dose for tizanidine a unique drug delivery method was created to address these challenges. Recent studies have demonstrated that the skin is a viable pathway for delivering drugs into the bloodstream [27]. Transdermal delivery has been selected due to its ability to maintain a consistent drug concentration in the bloodstream. The formulation of a transdermal drug delivery system can enhance its duration of action and minimize adverse effects, making it the most effective non-oral method for systemic drug administration [28] vesicular carriers, such as cubosomes, have been studied for their potential in transdermal drug administration to improve the penetration of drugs into the stratum cornium [29]. Based on tizanidine pharmacokinetic limitations namely, low oral bioavailability, being subject to significant first-pass metabolism in the liver, and possessing a short elimination half-life, tizanidine is considered a suitable candidate for transdermal drug delivery using cubosomal nanocarriers. This delivery strategy offers the potential to sustain therapeutic plasma levels, minimize dosing frequency, and improve patient compliance.

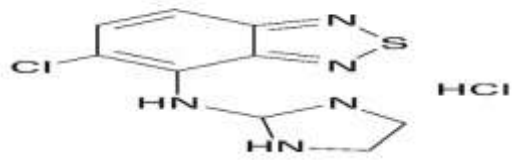

Figure 2. Chemical structure of tizanidine HCl [30]

Materials and Methods

Materials

TZN and glyceryl monooleate, Poloxamer 407 (Hyper chem company, China), PVA polymer (Hi media, India),) ethanol HPLC grade, chloroform AR grade (Chem-lab, Belgium), potassium

dihydrogen phosphate, sodium hydroxide, dialysis membrane with a molecular weight cut-off of 8–14 kDa (Lab Pvt Ltd., USA)

Study Design

Based on the data presented in Figure 3, GMO oil and Poloxamer P407 levels were selected as independent variables, and their effects on vesicle size, polydispersity index, and entrapment efficiency were statistically evaluated. The significance of each factor was assessed considering p-values less than 0.05 as statistically significant.

A Central Composite experimental model was formulated using Design Expert® version 13 (Stat-Ease, Inc., USA), where the independent variables were glyceryl monooleate (GMO) oil concentration (mg) and poloxamer 407 (P407) stabilizer concentration (mg). The primary responses investigated in this study were vesicle size, PDI and entrapment efficiency with the factor ranges determined based on prior literature.

Table 1 outlines the selected upper and lower limits of the independent variables, along with the defined response criteria. To ensure consistency during the preparation of TZN-loaded cubosomal nanovesicles, the drug concentration was maintained at 1.0 mg/mL throughout the preparation process.

Preparation of TZN-loaded cubosomal nano vesicle formulations

Cubosomes were created using the film hydration method. specifically, 10mg of TZN along with varying quantities of GMO (100-200 mg) and P407 (6-24mg), as detailed in table 2, were completely mixed with 3 mL of ethanol, the organic solvent was eliminated through vacuum-assisted evaporation with a rotary evaporator (Heidolph, Germany), resulting in the formation of a uniform lipid-polymer film composed of GMO and P407. Subsequently, this dry film was then hydrated with 10 mL of phosphate buffer solution with a PVA concentration of 1.25% w/v at a temperature of 70 ± 2°C. The dispersions were then subjected to sonication using a probe sonicator (Bandelin electronic, Germany) for a duration of 3 minutes. the sonicator was operated with a pulse mode, where it was turned off for 2 seconds and then turned on for 2-second intervals. The cubosomes dispersions were agitated for a duration of 2 hours and thereafter brought down to the ambient temperature. Afterwards, the samples were stored in glass vials at room temperature for further examination [31].

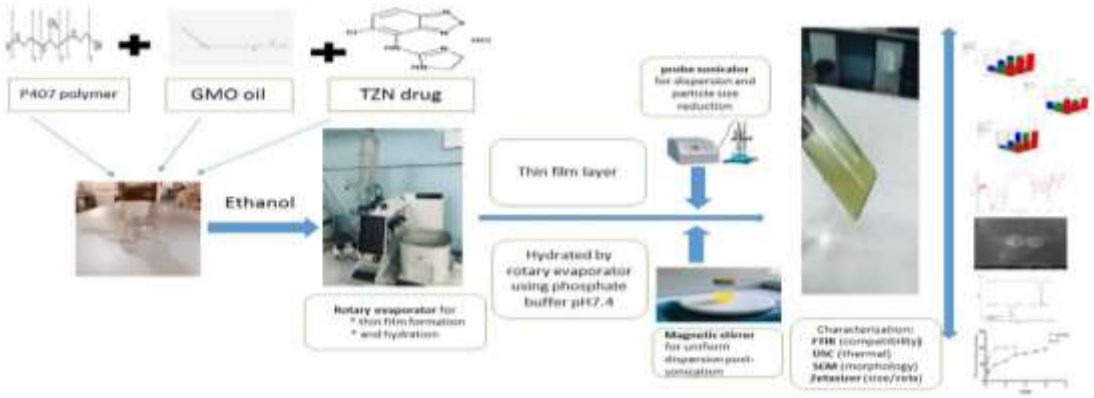

Figure 3. The graphical abstract for cubosomes nano vesicles formulation according to formulation component, method, and characterization

Table 1. Variables employed in the experimental design of Design Expert.

Variables	Symbols	Levels	Low	medium	high
Glyceryl monooleate GMO (mg)	A		100	150	200
poloxamer p407 (mg)	B		6	12	24
Particle size	Y1		Minimize		
Polydispersity index	Y2		Minimize		
Encapsulation efficiency (%)	Y3		Maximize		

Evaluation of Cubosomes Nano Vesicle Formulation

Measurement of the particle size and polydispersity index of the cubosomes

The particle size of the cubosomes was evaluated through the dynamic light scattering analysis employing a particle characterization instrument (Zetasizer 3000, Malvern, UK)). The polydispersity index (PDI) was also computed [32]. Before analysis, the formulations were diluted tenfold in deionized water.

***Entrapment efficiency* (EE%)**

The entrapment efficiency of TZN in cubosomal vesicles was measured using the ultrafiltration method, which involved quantifying the concentration of the drug that remained un

encapsulated in the supernatants [33]. 4 mL of the dispersion was transferred into the upper chamber of a microcentrifuge filter tube (Amicon® Ultra, 10 kDa molecular weight cut-off; Ireland) for centrifugation. The solution is thereafter subjected to centrifugation at a speed of 6,000 revolutions per minute for a duration of 10 minutes. To accurately determine the quantity of free unentrapped substances, it is necessary to dilute the ultra-filtrate with ethanol in a suitable manner. Absorbance measurements were carried out using Shimadzu ultraviolet spectrophotometer, at 319 nm [34]. Subsequently, tizanidine-free cubosomes (plain cubosomes) were utilized as blank samples. The percentage of encapsulation efficiency for tizanidine in cubosomes was determined based on the following equation [35]:

$$EE\% = \left(\frac{\text{Total amount of drug added - free drug}}{\text{Total amount of drug added}}\right) \times 100 \quad (1)$$

Drug Content Determination (% Assay)

To determine the drug content of the prepared formulation, a 1ml sample of the cubosomal dispersion containing 1mg of tizanidine was precisely taken and diluted with ethanol as the solvent. The sample absorbance was recorded at 319 nm using a UV-Visible spectrophotometer, with a solvent blank as the reference. The drug content was subsequently calculated based on the obtained absorbance values [36].

$$\text{Drug content} = \left(\frac{\text{Analyzed content}}{\text{Theoretical content}}\right) \times 100 \quad (2)$$

Zeta potential measurement

The electrophoretic mobility of the selected formulation was determined using a Zetasizer Nano ZS (Malvern Instruments, UK). The zeta potential was subsequently calculated to assess dispersion stability and the degree of electrostatic repulsion between charged particles. Prior to measurement, cubosomal nanovesicle samples were diluted tenfold with distilled water to achieve a uniform dispersion. the zeta potential was determined at 25 °C using a disposable zeta-type cuvette. each measurement was conducted in triplicate, and the results were recorded accordingly [35].

Scanning electron microscopy (SEM)

Examining the morphology of the improved formulation using scanning electron microscopy scanning electron microscopy was utilized to ascertain the morphology of the improved formulation Morphological characterization was conducted on the dried samples by dispersing aa small quantity onto aluminum stubs. The samples were then coated with a thin layer of gold and the samples were examined under an argon atmosphere using a scanning electron microscope operated at an accelerating voltage of 30 kV, and representative images were subsequently captured [37].

Differential scanning calorimetry (DSC)

Differential scanning calorimetry (DSC) was conducted on both the pure drug and the optimized formula to determine the thermal compatibility between the drug and polymer during the formulation of cubosomes, as well as to evaluate the crystalline state of the drug [38]. A differential scanning calorimetry (DSC) study was conducted on the drug and its improved formula using a DSC-600 instrument manufactured by Shimadzu in Japan. approximately 5 mg of the sample, consisting of both the pure drug and the improved formula, were inserted and sealed in separate aluminum pans using external pressure. The aluminum pans were heated from 0°C to 400°C using a nitrogen flow rate of 30 ml/min to create an inert environment. the heating was done at a scanning rate of 10°C/min [39].

Fourier transform infrared spectroscopy (FTIR) study

The IR spectra of the drug, the drug combined with excipients (physical mixture), and the optimized formula were obtained in a solid state by creating a pellet using potassium bromide (KBr). the spectra were obtained by scanning the produced KBr pellets using an FTIR spectrometer, within a wavelength range of 4000–400 cm^{-1} [40].

X-ray diffraction (XRD) analysis

X-ray diffraction analysis of the pure drug and optimized formulation was performed using an XRD-6000 diffractometer (Shimadzu, Japan), operated at 40 kV and 30 mA, employing Cu-Kα radiation. with a wavelength of $\lambda = 1.5406$ nm. The scanning speed was set at 5°/min over a 2θ range of 0 to 60°. Each sample was scanned individually [41].

In-vitro drug release study

The release behavior of the drug was investigated employing the dialysis membrane diffusion method. a dialysis membrane with a molecular weight cut off range of (8000-14000) Da was employed in a USP dissolution apparatus type II. To maintain sink conditions, 500 mL of phosphate buffer solution (pH 7.4) was used as the dissolution medium. The experiment was conducted at a controlled temperature of 37 ± 0.5°C, with a constant stirring speed of 50 rpm, samples of 5 mL were withdrawn at predetermined time intervals of 0.25, 0.5, 1, 2, 3, 4, 6, 8, and 12 hours. An equal volume of fresh medium was immediately added to maintain sink conditions. the absorbance of the collected samples was then analyzed, and drug concentration was quantified accordingly [42]

Kinetic models

The release profiles of the optimized cubosomal formulations were subjected to kinetic analysis. This evaluation was conducted using Microsoft Excel® 2016 in combination with the DDsolver add-in to identify the most appropriate release mechanism and he most suitable mathematical model governing the release of

tizanidine from cubosomal formulations. This analysis involved fitting the release data to four conventional kinetic models: zero-order, first-order, higuchi, and korsmeyer-Peppas kinetics [43].

Results and Discussion

Evaluation of the Central Composite Design for TZN-Loaded Cubosomal Nanovesicles

The formulation compositions and their corresponding experimental responses, including particle size (PS), polydispersity index (PDI), and entrapment efficiency (EE%), are summarized in Table 2. These formulations were developed using a central composite design. Analysis of the regression coefficients provided valuable insights into the influence of the independent variables on the measured responses. Furthermore, the three-dimensional (3D) response surface plots in Figure 4 illustrate how the concentrations of glyceryl monooleate (GMO) oil and Poloxamer 407 polymer affect the PDI, EE%, and particle size of the cubosomal nanovesicles**.**

Particle size/PDI analysis

Particle size analysis revealed that the TZN-loaded cubosomes exhibited sizes ranging from 113.5 to 182.6 nm, as shown in Table 2. A linear model was identified as the best fit for describing the particle size response. The model demonstrated statistical significance, indicated by an F-value of 18.53. Additionally, the predicted R^2 value (0.6432) was reasonably close to the adjusted R^2 value (0.8142), with a difference of less than 0.2, the adequate precision value, which reflects the signal-to-noise ratio, was 12.042 substantially exceeding the desirable threshold of 4, confirming that the model provides an adequate signal. Furthermore, the p-values for terms A and B were found to be significant, as their values were less than 0.05. Specifically, the p-values were 0.0037 and 0.0072 for factors A and B, respectively.

$$Partical\ size = 154.33 + 17.32 \times A - 14.75 \times B \quad (3)$$

The equation represents the relationship between the amount of GMO (A) and the amount of P407 (B). A positive coefficient reflects a synergistic contribution to increasing the response, whereas a negative coefficient suggests an antagonistic effect.

The analysis confirmed that the cubosomal vesicle size was significantly influenced by both the amount of GMO and the concentration of P407 ($p < 0.05$), as demonstrated in Figure 5. Notably, increasing the concentration of P407 polymer resulted in a significant reduction in vesicle size, which is consistent with findings previously reported by Rash et al. [44]. The capacity of P407 polymer as a surfactant to decrease surface tension might be attributed to this phenomenon. This resulted in a reduction in the surface energy of the cubosomes, hence inhibiting the aggregation of particles. conversely, the inadequate quantity of emulsifier was unable to effectively stabilize all nanoparticles, leading to their coalescence [45]. The quantity of surfactant is crucial in both the emulsification process and the prevention of droplet aggregation. As larger size cubosomal nanoparticles were obtained upon reducing poloxamer concentration Figure 4; p407 stabilizers are employed to alter the surface characteristics of cubosomes, hence enhancing their stability. The stability of the lipid nanostructure is achieved by effectively insulating it from the surrounding aqueous media [46]. It was found that the size of the particles increased significantly ($p<.005$) as the concentration of GMO oil increased, an increase in the lipid phase concentration is likely to lead to an elevation in dispersion viscosity, which can impede the breakdown of the produced bicontinuous structures into smaller sizes [47], Similar result was found by Eldeeb et al. in their study on the development and assessment of cubosomes as a medication delivery system for the treatment of glaucoma [48].

Table 2. Physicochemical characteristics of different tizanidine loaded cubosomes.

Formulations code	Factor1	Factor2	Response 1	Response 2	Response 3	
	GMO	P407	Particle size (nm)	Poly dispersity index	Encapsulation efficiency (%)	Total drug content %
F1	100	6	165	0.135	72.09	98.5
F2	150	6	171.2	0.3011	73.4	99.4
F3	200	6	182.6	0.1777	79.2	99.7
F4	100	12	134.1	0.1198	69.04	100.2
F5	150	12	153.1	0.08549	71.24	99.4
F6	200	12	173.2	0.141	77.2	100.05
F7	100	24	113.5	0.109	67.09	99.8
F8	150	24	150.3	0.1125	69.94	100.3
F9	200	24	160.7	0.061	76.8	99.8

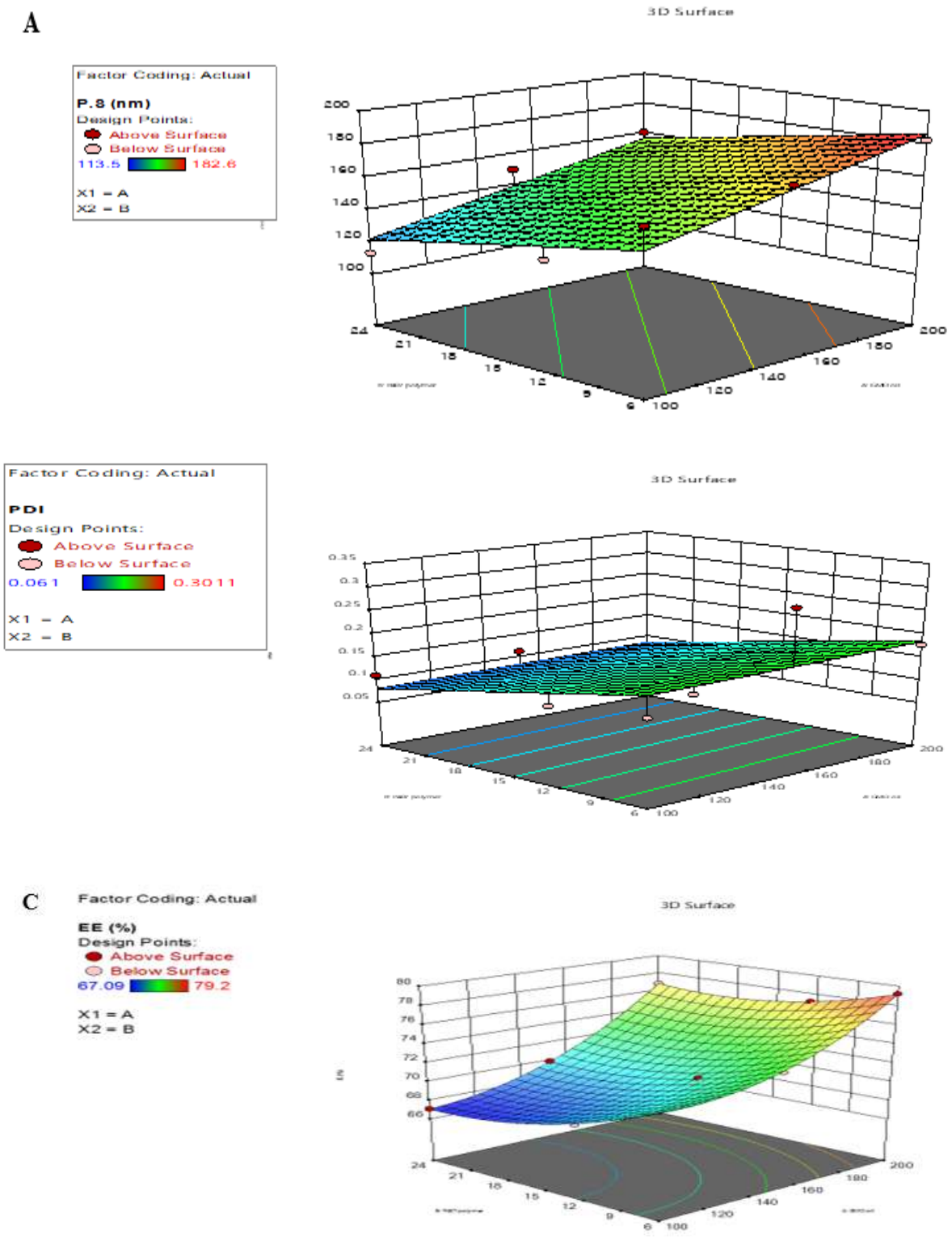

Figure 4. 3D-response charts expressive the effect of independent variables on (A) P.S (B) PDI, and (C) EE%

The polydispersity index (PDI) varied between 0.049 and 0.3011. PDI is defined as the square root of the ratio between the standard deviation and the mean particle diameter. The range of values for the PDI is between (0 and 1), PDI larger than 0.5 indicates that the formulation is not uniform [49,50]

For the PDI response, a linear model was applied. However, the model's F-value of 1.97 indicates a lack of statistical significance in explaining particle

size distribution. This conclusion is further supported by a negative predicted R^2 (-0.136), a relatively low adjusted R^2 of 0.1955, and an adequate precision value below the acceptable threshold of 4 (recorded at 2.9017). Furthermore, the p-values associated with factors A and B were found to be statistically insignificant (p = 0.920 and 0.094, respectively), as they exceeded the 0.05 significance level.

Equation (4) was utilized to determine the potential influence of each factor's specific level on PDI.

$$PDI = +0.1326 + 0.00265 \times A - 0.0496 \times B \quad (4)$$

The study reveal indicates that particle size distribution was decrease by the increase in concentration p407 (Fgure 6) the effect is insignificant (p> 0.005). The effect of p407 on particle size distribution may be attributed to the same mechanism previously discussed for its effect on particle size.

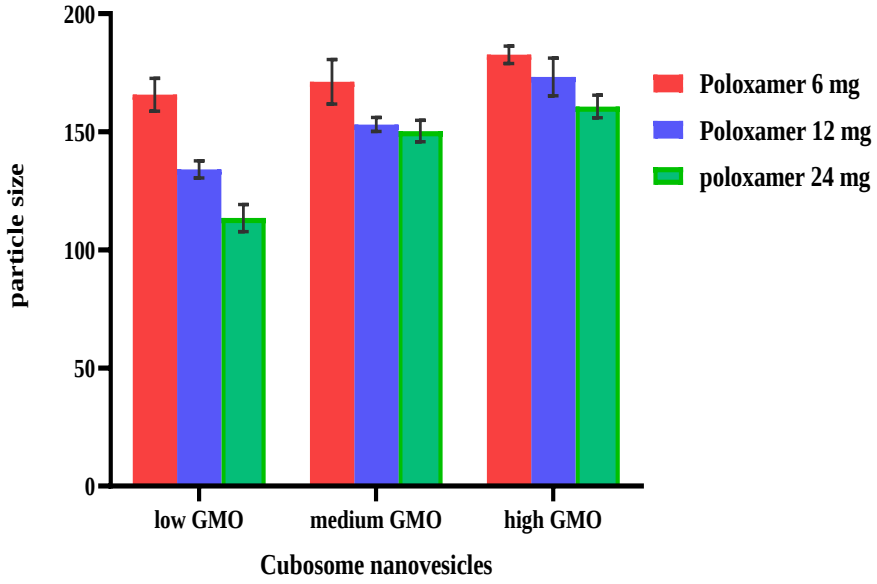

Figure 5. Effect of GMO oil and poloxamer p407 concentrations on particle size

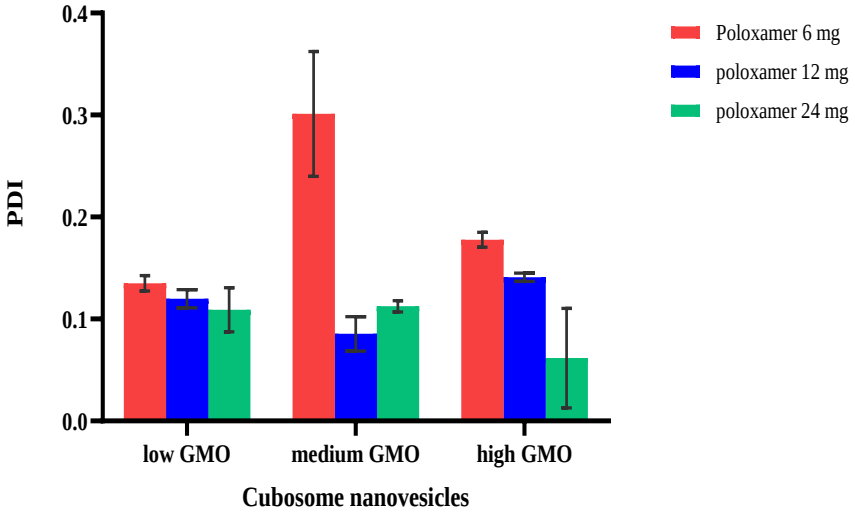

Figure 6. Effect of GMO oil and poloxamer p407 concentrations on PDI

Entrapment efficiency analysis

A quadratic model was found to best fit the entrapment efficiency (EE%) response. As presented in Table 2, the encapsulation efficiency of tizanidine-loaded cubosomes ranged from 67.09% to 79.2%, indicating substantial drug loading capacity. The statistical analysis yielded a model F-value of 1422.8, confirming the model's significance in predicting entrapment efficiency. The predicted R^2 value of 0.9965 was in close agreement with the adjusted R^2 value of 0.9988, with a difference less than 0.2, indicating the model's reliability. Moreover, the adequate precision value was 107.7, exceeding the desirable threshold of 4, further supporting the model's adequacy. Additionally, the p-values for the main factors (A and B), their interaction (AB), and the quadratic terms (A^2 and B^2) were all statistically significant, with values less than 0.05. Specifically, the p-values were <0.0001 for A and B, 0.0024 for AB, 0.0002 for A^2, and 0.0012 for B^2. Equation 5 provides an understanding of how the formulation parameters affect the (EE%).

$$EE = +70.38 + 4.23 * A - 1.81 * B + 0.64 * AB + 2.043 * A^2 + 1.34 * B^2 \quad \ldots\ldots \quad (5)$$

The results demonstrated that increasing the GMO oil content positively influenced the entrapment efficiency, but the presence of p407 had an adverse effect the analysis showed that (EE) of cubosomes were significantly affected by P407as well as the amount of GMO ($P < 0.05$). The reduction in EEs seen with increasing P407 concentration may be attributed to the surfactant properties of P407, which enhance the drug's solubility in the surrounding environment, resulting in the leakage of the drug into the release medium [51,52]. Furthermore, the combination of decreasing the concentration of P404 and increasing the quantity of lipids led to an accelerated solidification of the cubosomal nanoparticles. This might be attributed to the heightened viscosity of the medium. furthermore, this would inhibit the spread of drugs to the outer phase of the medium [44].

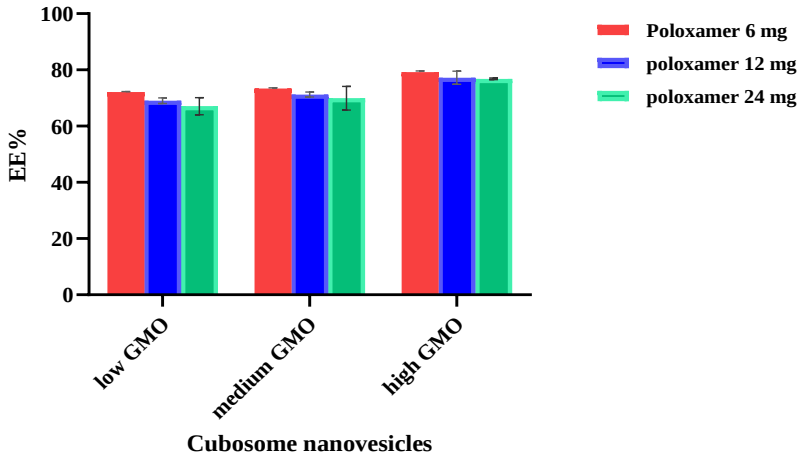

Figure7. Effect of GMO oil and poloxamer p407 concentrations on entrapment efficiency

Total drug content (% assay)

The drug content study showed that the average percentage of drug content in the formulations ranged from 98.524±0.012% to 100.308±0.013%, as stated in Table 2. the results were consistent with the requirements set by the United States Pharmacopeia (USP) [53]. indicating a high degree of appropriateness in the production technique**.**

Optimization

A computer-aided formulation optimization process was conducted using the Design Expert® software, employing the desirability approach to evaluate the influence of varying levels of the independent factors on the measured outcomes. The acceptance criteria for the responses were set as follows: vesicle size ranging from 113.5 to 182.6 nm (Y1), polydispersity index (PDI) between 0.049 and 0.3011 (Y2), and entrapment efficiency (EE%) from 67.09 to 79.2% (Y3). The target was established to be within the minimal value for particle size, PDI and with the greatest value of EE based on the results obtained in this research study. The formulation that demonstrated the best compromise, with an overall desirability score of 62.6%, was selected and prepared using 200 mg of GMO and 24 mg of Poloxamer 407 (F9). Table 3 summarizes both the predicted and experimentally observed values for the optimized formulation's responses.

Table 3. Correlation between expected and observed response values of the optimized formulation

Tested Parameter	Vesicle Size (nm)	Size Distribution (PDI)	Encapsulation efficiency(%)
Actual values	160.7	0.061	76.8
Predicted	157.811	0.097	76.21
Absolute error%	1.83%	37.1	0.77%

Differential scanning calorimetry (DSC)

The DSC thermogram of tizanidine in Figure 8 for pure drug (red curve) has a distinct endothermic peak at 293.78°C, indicates the crystalline nature of the pure drug which aligns with the documented melting temperature range of tizanidine hydrochloride. [54]. The disappearance of the characteristic sharp melting peak of tizanidine at 293.78°C for optimized formula F9, (blue curve) suggests a loss of its crystalline nature, indicating potential amorphous or molecular dispersion within the formulation.

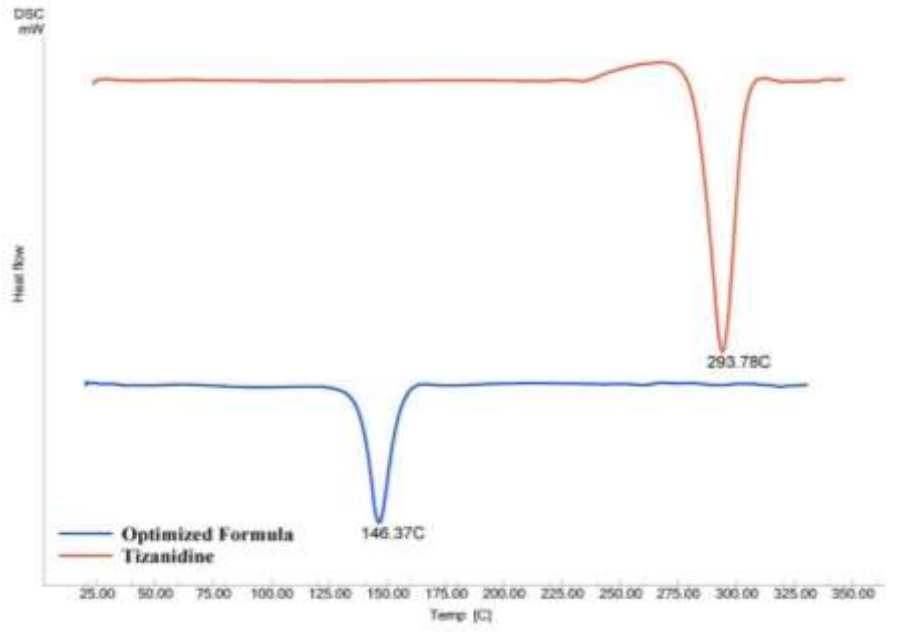

Figure 8. DSC thermogram –– pure tizanidine, and –– optimized formula

Fourier transform infrared spectroscopy (FTIR)

Figure 9 displays the FTIR spectra of tizanidine, its physical mixture with excipients, and the optimized formulation. Additionally, the spectrum of the pure drug was compared with the standard reference spectrum provided in the Japanese Pharmacopoeia 2017 [55] in table 4, the comparison revealed the presence of all characteristic peaks of functional groups of pure drug, which correspond to the distinctive peaks of tizanidine as shown in the spectra of reference, the shift in the N-H stretching peak (3244 cm^{-1} in pure drug → 3401 cm^{-1} in selected formula(F9) suggests hydrogen bonding between tizanidine and excipients (Poloxamer 407, GMO). The study's results suggest that there are no significant chemical interactions present [56].

Table 4. Fourier Transform Infrared (FTIR) Spectrum of the pharmaceutical compound tizanidine [55]

Functional Group / Vibration Type	Characteristic Absorption (cm^1)[54]	Observed Wavenumber (cm^{-1})
N–H stretching (secondary amine)	3100-3500	3244.56
C–H stretching (aromatic)	Just above 3000 (3000-3100)	3071.03
N–H bending (secondary amine)	1900	1938.1
C=C stretching (aromatic ring)	Typically appears as doublet at ~1600 & 1475	1605.45& 1438.96
C–N stretching (secondary amine)	1100-1300 & 700-900	1188.90 & 884.92
C–Cl stretching (aromatic)	1035-1100	1067.41
Ring bending	Strong band near 700	710.64

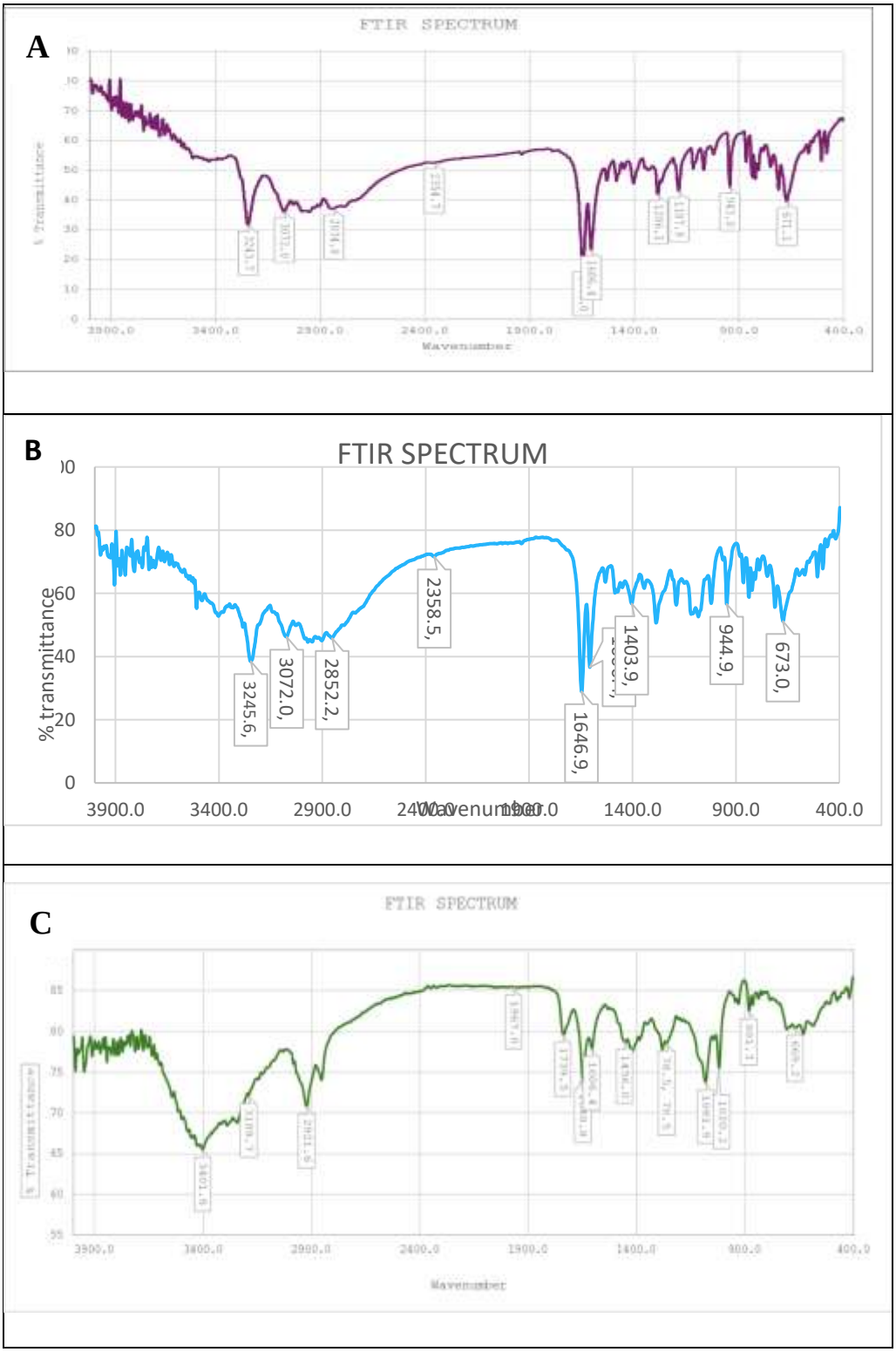

Figure 9. FTIR spectra of (A) pure tizanidine , (B) the drug–excipient physical mixture, and (C) the optimized formulation.

X-ray diffraction (XRD)

The XRD diffractograms of tested samples presented in Figure 10. XRD diffractogram of pure tizanidine confirms its crystalline nature, as evident from the number of sharp and intense peaks as it displayed sharp intense narrow diffraction peaks , additionally, optimize formula displayed no sharp peaks with lower intensity of characteristic peaks situated at 25° and 12° (2q) indicating amorphous structure of tizanidine within cubosomal formulation.

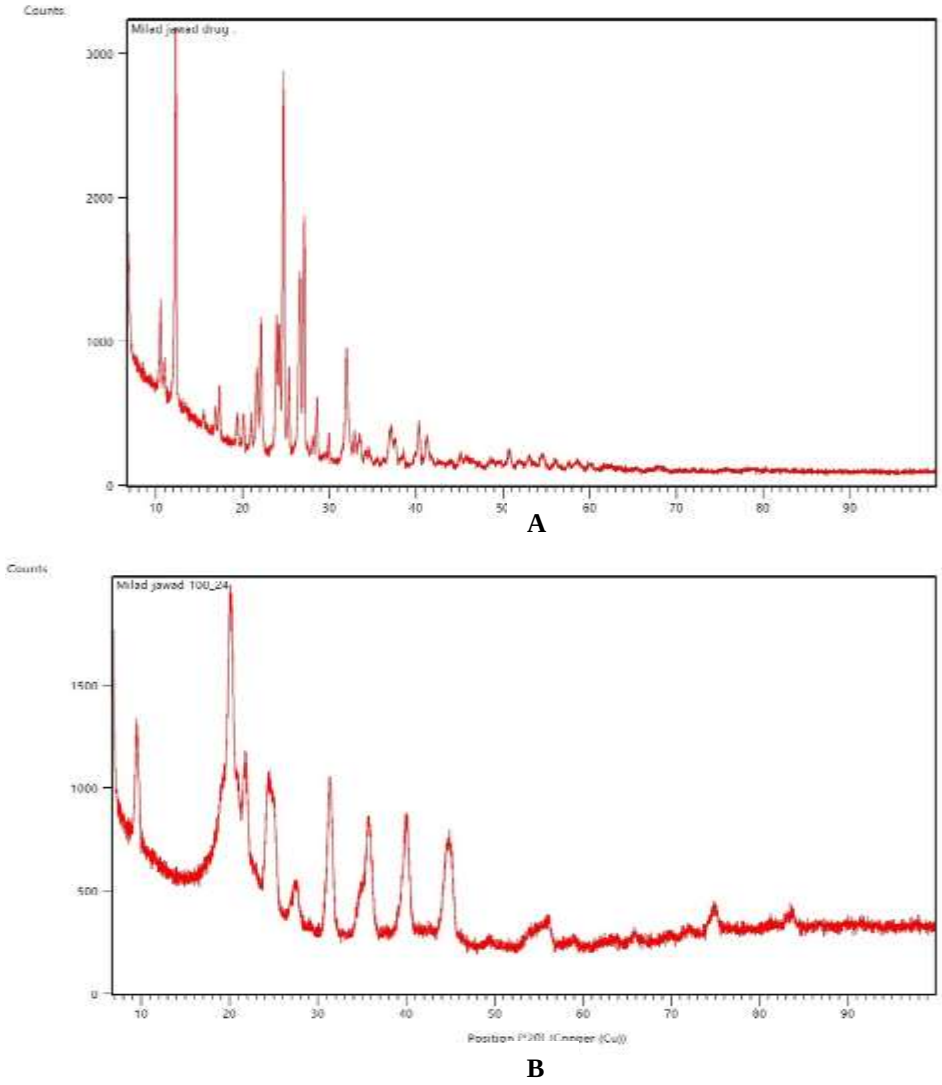

Figure 10. X-ray Diffraction Pattern of A) Pure Drug. B) Optimize the formula.

Zeta potential

A sufficiently high zeta potential, whether negative or positive, zeta potential can effectively prevent the aggregation of particles, thereby improving the stability of the dispersion. As the zeta potential becomes more negative, electrostatic repulsion between particles is enhanced, reducing the likelihood of particle aggregation [57]. The optimized formula (F9) yielded a value of -23.46 mV which is generally considered to reflect moderate stability. Although this value does not exceed the ±30 mV threshold for high stability, it still indicates sufficient electrostatic repulsion to prevent particle aggregation during storage. The negative surface charge on tzn loaded cubosomes may arise from the ionization of carboxylic groups present in GMO and adsorbed onto the surface of the cubosomes. Alternatively, this effect could be explained by the formation of a polarized water layer on the cubosome surface [58].

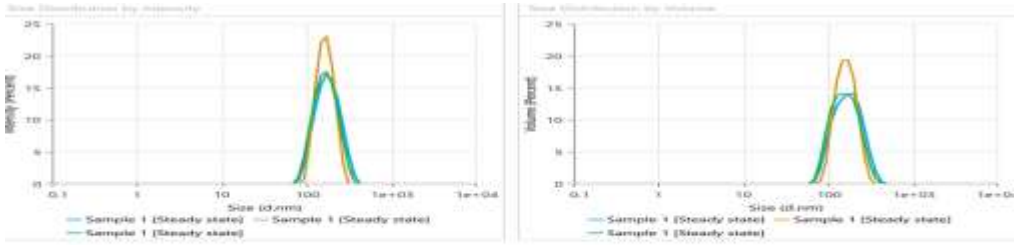

A

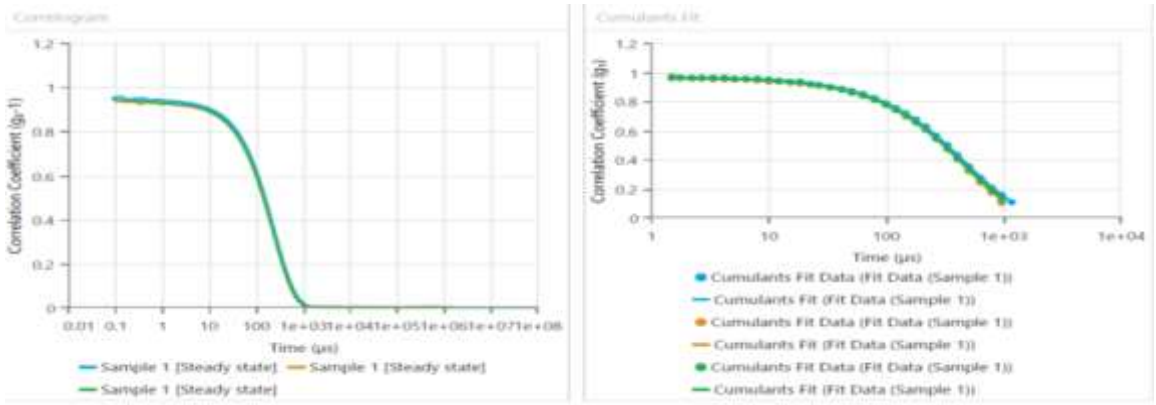

B

Figure 11. Particle size analysis of formulation F9 using the Malvern Zetasizer: (A) intensity distribution and (B) cumulative distribution curve

Scanning electron microscopy (SEM)

The surface morphology of the selected formulation, examined by scanning electron microscopy (SEM), is shown in Figure 12. The micrographs reveal that the prepared cubosomes were nano-sized particles exhibiting a cubic shape, uniform size distribution, good dispersion, and adequate separation between individual particles.

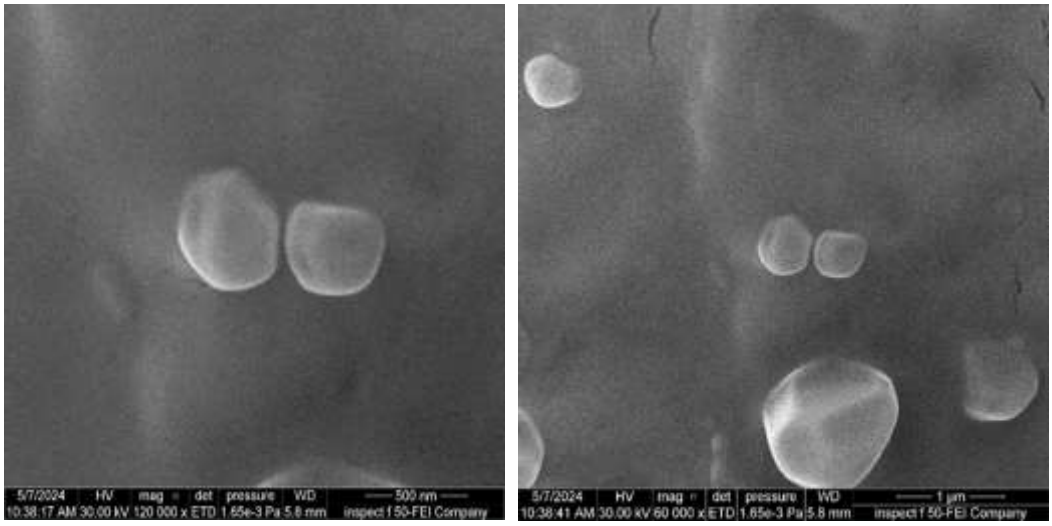

Figure 12. Characterization of the morphology of tizanidine-loaded optimized cubosomes using scanning electron microscopy.

In-vitro drug release

The in vitro release profile of tizanidine (TZN) from TZN-loaded cubosomes, in comparison with an aqueous solution of tizanidine (TZN), is presented in Figure 13. The aqueous solution of TZN exhibited a rapid and complete release within the first hour. conversely, the release profile of TZN from cubosomes demonstrated a biphasic pattern, characterized by an initial burst release of approximately 48.5% within the first hour, followed by a sustained and gradual release over the subsequent six hours. The pronounced initial burst release can be attributed to the weakly bound or adsorbed drug on the relatively larger surface area of the nanoparticles [59]. Similar burst release behavior has been previously reported for both hydrophilic and hydrophobic drugs encapsulated in cubosomes [60]. The sustained release of tizanidine (TZN) from cubosomes can be attributed to the restricted diffusion of drug molecules within the aqueous channels of the cubic phase. This diffusion process is primarily influenced by the tortuosity and the relatively small pore size of these channels, which hinder the movement of the drug [61]. Furthermore, the limited pore size of the dialysis membrane can impede the diffusion of nano vesicles, thereby resulting in a reduced release rate [62].

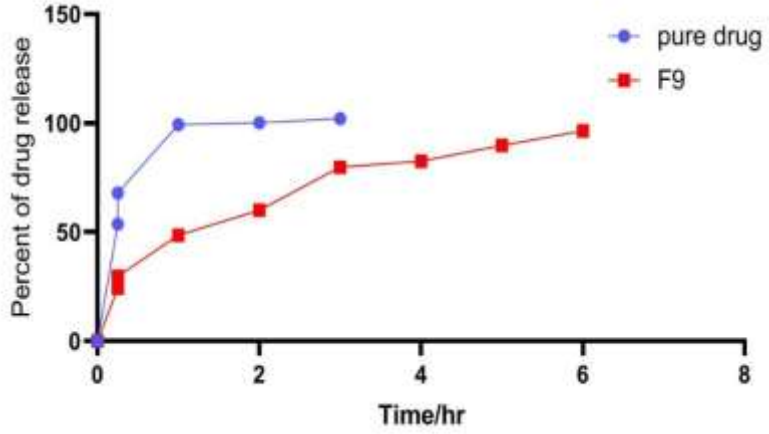

Figure 13. In-vitro drug release of pure drug solution and TZN loaded nano vesicle (F9) in phosphate buffer pH 7.4

Release kinetics modeling

The in vitro drug release behavior of tizanidine from different cubosomal preparations was analyzed by fitting the experimental data to different kinetic models. Table 4 outlines the calculated release rate constants along with the corresponding correlation coefficients (R^2) for each model applied. Among the evaluated models, the Korsmeyer–Peppas equation provided the best fit for describing the drug diffusion from the cubosomal systems, as evidenced by its superior R^2 values across all tested preparations. Comparable results were previously observed by Sabri et al. in their study on drug release from spanlastic carriers [43].

Table 4. In vitro release kinetics data of tizanidine

Formula code	Zero-order		First order		Higuchi model		Korsmeyer-Peppas model		
F9	K_0	R^2	K1	R^2	kH	R^2	Kkp	n	R^2
	19.577	0.4311	0.546	0.9444	41.702	0.9695	45.69	0.429	0.9850

Conclusion

This study explores the formulation of tizanidine (TZN) as cubosomal nanovesicles using the thin-film evaporation method. The findings indicate that formulation F9 exhibits optimal characteristics displaying favorable vesicle size, polydispersity index, and entrapment efficiency, with no observed interactions between the drug and excipients. Furthermore, photomicrographs of the prepared cubosomes demonstrate a uniform cubic morphology, suggesting an improved capacity for controlled drug released, the proposed system can be efficiently utilized for transdermal drug delivery systems to control the release of tizanidine it is expected to optimize bioavailability.

Acknowledgment

We extend our appreciation to the University of Baghdad, College of Pharmacy for providing the

laboratory facilities, materials, and instrumentation necessary to complete this research. No specific grant number was assigned to this project.

Conflict of Interests

The authors declare that there were no conflicts of interest regarding the publication of this paper.

Funding

The authors confirm that no financial support was received for conducting this research or preparing the manuscript.

Ethics Statements

This study was conducted entirely in vitro; therefore, ethical approval was not required

Author Contribution

The authors contributed to this work as follows: study conception and design were carried out by Nawal Ayash Rajab. Experimental procedures, data analysis, interpretation of results, and initial manuscript drafting were performed by Milad Jawad Hasan. Both authors critically revised the manuscript and approved its final version for submission.

References

1. Gupta L, Mittal A, Katrolia A, Raizaday A, Kaushik L, Shukla BK. Cubosomes: the pliant honeycombed nano-cargos in drug delivery applications. Nanomedicine J. 2024;11(2):1–18.
2. Bachhav AA, Pingale PL, Upasani CD, Ahire SA. Cubosome: a novel vesicular drug delivery system. Int J Pharm Sci Res. 2024;15(2):323–339.
3. Attri N, Shabbir M, Ali S, Hamid I, Sharif A, Akhtar MF, et al. Liposomes to cubosomes: the evolution of lipidic nanocarriers and their cutting-edge biomedical applications. ACS Appl Bio Mater. 2024;7(5):2677-2694. doi:10.1021/acsabm.4c00153.
4. Zhai J, Fong C, Tran N, Drummond CJ. Non-lamellar lyotropic liquid crystalline lipid nanoparticles for the next generation of nanomedicine. ACS Nano. 2019;13(6):6178–6206. doi:10.1021/acsnano.8b07961.
5. Sivadasan D, Sultan MH, Alqahtani SS, Javed S. Cubosomes in drug delivery—a comprehensive review on its structural components, preparation techniques and therapeutic applications. Biomedicines. 2023;11(4).
6. Garg G, Saraf S, Saraf S.Cubosomes: An Overview.Cubosomes: an overview.Biol Pharm Bull. 2007;30(2):350-353.
7. Chacko IA, Ghate VM, Dsouza L, Lewis SA. Lipid vesicles: a versatile drug delivery platform for dermal and transdermal applications. Colloids Surf B Biointerfaces. 2020;195:111262. doi:10. 1016/ j. colsurfb .2020.111262.
8. Urandur S, Marwaha D, Gautam S, Banala VT, Sharma M, Mishra PR. Nonlamellar liquid crystals: a new paradigm for the delivery of small molecules and bio-macromolecules. Ther Deliv. 2018;9(9):667-689.
9. Khedekar PB. Cubosomes: a vehicle for delivery of various therapeutic agents. MOJ Toxicol. 2018;4(1).
10. Li JC, Zhu N, Zhu JX, Zhang WJ, Zhang HM, Wang QQ, et al. Self-assembled cubic liquid crystalline nanoparticles for transdermal delivery of paeonol. Med Sci Monit. 2015;21:3298-3310.
11. Hasan MJ, Rajab NA. Nano vesicular topical drug delivery system: types, structural components, preparation techniques, and characterizations. J Emerg Med Trauma Acute Care. 2024;(6):16.
12. Zakaria F, Ashari SE, Mat Azmi ID, Abdul Rahman MB. Recent advances in encapsulation of drug delivery (active substance) in cubosomes for skin diseases. J Drug Deliv Sci Technol. 2022;68:103097. doi:10.1016/j.jddst.2022.103097.
13. Kaur SD, Singh G, Singh G, Singhal K, Kant S, Bedi N. Cubosomes as potential nanocarrier for drug delivery: a comprehensive review. J Pharm Res Int. 2021;33(31B):118–135. doi:10.9734/jpri/2021/v33i31b31698.
14. Chaudhary K, Sharma D. Cubosomes: a potential drug delivery system. Asian J Pharm Res Dev. 2021;9(5):93–101
15. Garg M, Goyal A, Kumari S. An update on the recent advances in cubosome: a novel drug delivery system. Curr Drug Metab. 2021;22(6):441–450.
16. Katekar VA, Deshmukh SP, Borkar RD, Rathod HK. Cubosome: an overview. J Surv Fish Sci. 2023;10(1):4397–4411.
17. Hartnett TE, O'Connor AJ, Ladewig K. Cubosomes and other potential ocular drug delivery vehicles for macromolecular therapeutics. Expert Opin Drug Deliv. 2015;12(9):1513–1526.
18. Peng X, Zhou Y, Han K, Qin L, Dian L, Li G, et al. Characterization of cubosomes as a targeted and sustained transdermal delivery system for capsaicin. Drug Des Devel Ther. 2015;9:4209–4218.
19. Mukherjee A, Chakravarty A. Spasticity mechanisms – for the clinician. Front Neurol. 2010 Mar;.
20. Wieters F, Weiss Lucas C, Gruhn M, Büschges A, Fink GR, Aswendt M. Introduction to spasticity and related mouse models. Exp Neurol. 2021;335:113491
21. Ghai A, Garg N, Hooda S, Gupta T. Spasticity - pathogenesis, prevention and treatment strategies. Saudi J Anaesth. 2013;7(4):453–460.

22. Chou R, Peterson K, Helfand M. Comparative efficacy and safety of skeletal muscle relaxants for spasticity and musculoskeletal conditions: a systematic review. J Pain Symptom Manage. 2004;28(2):140–175. doi:10. 1016 /j. jpain symman .2004.05.002.

23. Wagstaff AJ, Bryson HM. Tizanidine: a review of its pharmacology, clinical efficacy and tolerability in the management of spasticity associated with cerebral and spinal disorders. Drugs. 1997;53(3):435–452. doi:10.2165/00003495-199753030-00007.

24. Fadhel AY, Rajab NA. Tizanidine nano emulsion: formulation and in-vitro characterization. J Pharm Negative Results. 2022;13(3):572–581.

25. Peck J, Urits I, Crane J, McNally A, Noor N, Patel M, et al. Oral muscle relaxants for the treatment of chronic pain associated with cerebral palsy. Psychopharmacol Bull. 2020 Oct 15;50(4 Suppl 1):142–162. PMID: 33633423; PMCID: PMC7901132.

26. Arpa MD, Üstündağ Okur N, Gök MK, Cevher E. Chitosan-based buccal mucoadhesive bilayer tablets enhance the bioavailability of tizanidine hydrochloride by bypassing the first-pass metabolism. J Drug Deliv Sci Technol. 2024;105739.

27. Noor AH, Ghareeb MM. Formulation and evaluation of ondansetron HCl nanoparticles for transdermal delivery. Iraqi J Pharm Sci. 2020;29(2):70–79.

28. Shaik NB, Mortha SD, Lakshmi PK, Kukati L. Formulation and evaluation of tizanidine hydrochloride loaded ethosomes for transdermal delivery. J Pharm Sci Res. 2020;12(11):1400–1410

29. lbassam NY, Kassab HJ. Diacerein loaded novasome for transdermal delivery: preparation, in-vitro characterization and factors affecting formulation. Iraqi J Pharm Sci. 2023;32(Suppl):214–224.

30. Shabbir M, Sajid A, Hamid I, Sharif A, Akhtar MF, Raza M, et al. Influence of different formulation variables on the performance of transdermal drug delivery system containing tizanidine hydrochloride: in vitro and ex vivo evaluations. Braz J Pharm Sci. 2019;54:e00130.

31. Zaker H, Taymouri S, Mostafavi A. Formulation and physicochemical characterization of azithromycin-loaded cubosomes. Res Pharm Sci. 2023;18(1):49–58. doi:10.4103/1735-5362. 363 595.

32. Al-Tamimi DJ, Hussein AA. Formulation and characterization of self-microemulsifying drug delivery system of tacrolimus. Iraqi J Pharm Sci. 2021;30(1):91–100.

33. Ali SK, Al-Akkam EJ. Effects of different types of bile salts on the physical properties of ropinirole-loaded formulations. Al-Rafidain J Med Sci. 2023;5:134–142.

34. Mohsen AM, El-Hashemy HA, Salama A, Darwish AB. Formulation of tizanidine hydrochloride–loaded provesicular system for improved oral delivery and therapeutic activity employing a 2^3 full factorial design. Drug Deliv Transl Res. 2023;13(2):580–592.

35. Alkufi HK, Kassab HJ. Soluplus-stabilized nimodipine-entrapped spanlastic formulations prepared with edge activator (Tween 20): comparative physicochemical evaluation. Pharm Nanotechnol. 2025;13(3):551–563. doi:10. 2174 / 0122117385348551241028102256.

36. Ghareeb MM. Formulation and characterization of isradipine as oral nanoemulsion. Iraqi J Pharm Sci. 2020;29(1):143–153.

37. Mansour M, Kamel AO, Mansour S, Mortada ND. Novel polyglycerol-dioleate based cubosomal dispersion with tailored physical characteristics for controlled delivery of ondansetron. Colloids Surf B Biointerfaces. 2017;156:44–54.

38. Ibraheem FQ, Al-Gawhri FJ. Preparation and in-vitro evaluation of baclofen as an oral microsponge tablet. Iraqi J Pharm Sci. 2019;28(1):75–90.

39. Fareed NY, Kassab HJ. Studying the effect of variables on acyclovir microsponge. Iraqi J Pharm Sci. 2018;66–76.

40. Kala S, Juyal D. Preformulation and characterization studies of aceclofenac active ingredient. Pharma Innov. 2016;5(9, Part B):110.

41. Abdulbaqi MR, Rajab NA. Preparation, characterization and ex vivo permeability study of transdermal apixaban O/W nanoemulsion-based gel. Iraqi J Pharm Sci. 2020;29(2):214–222.

42. Nashat BI, Al-Kinani KK. Nanoemulsion formulation of leflunomide for transdermal delivery: preparation and characterization. Int J Drug Deliv Technol. 2023;13(1):57–65.

43. Sabri L, Khalil M. Impact of formulation variables on meloxicam spanlastics preparation. Iraqi J Pharm Sci. 2024;33(4):59–68.

44. Alkawak RSY, Rajab NA. Lornoxicam-loaded cubosomes: preparation and in vitro characterization. Iraqi J Pharm Sci. 2022;31(1):144–153.

45. Amanat S, Taymouri S, Varshosaz J, Minaiyan M, Talebi A. Carboxymethyl cellulose-based wafer enriched with resveratrol-loaded nanoparticles for enhanced wound healing. Drug Deliv Transl Res. 2020;10:1241–1254.

46. Mainardes RM, Evangelista RC. PLGA nanoparticles containing praziquantel: effect of formulation variables on size distribution. Int J Pharm. 2005;290(1-2):137–144.

47. Elgindy NA, Mehanna MM, Mohyeldin SM. Self-assembled nano-architecture liquid crystalline particles as a promising carrier for progesterone transdermal delivery. Int J Pharm. 2016;501(1-2):167–179.

48. Eldeeb AE, Salah S, Ghorab M. Formulation and evaluation of cubosomes drug delivery system for treatment of glaucoma: ex-vivo permeation and in-vivo pharmacodynamic study. J Drug Deliv Sci Technol. 2019;52:236–247.

49. aymouri S, Varshosaz J, Hassanzadeh F, Haghjooy Javanmard S, Dana N. Optimization of processing variables effective on self-assembly of folate targeted Synpronic-based micelles for docetaxel delivery in melanoma cells. IET Nanobiotechnol. 2015;9(5):306–313.

50. Varshosaz J, Hassanzadeh F, Sadeghi-Aliabadi H, Firozian F. Uptake of etoposide in CT-26 cells of colorectal cancer using folate-targeted dextran stearate polymeric micelles. Biomed Res Int. 2014;2014:1–9.

51. Morsi NM, Mohamed MI, Refai H, El Sorogy HM. Nanoemulsion as a novel ophthalmic delivery system for acetazolamide. Int J Pharm Pharm Sci. 2014;6(11):227–236.

52. Teba HE, Khalil IA, El Sorogy HM. Novel cubosome-based system for ocular delivery of acetazolamide. Drug Deliv. 2021;28(1):2177–2186. doi:10.1080/10717544.2021.1989090.

53. The United States Pharmacopeia and National Formulary (USP 44, NF 39). Rockville, MD: United States Pharmacopeia Convention Inc; 2021.

54. Jagdale S, Brahmane S, Chabukswar A. Optimization of microemulgel for tizanidine hydrochloride. Anti-Inflamm Anti-Allergy Agents Med Chem. 2020;19(2):158–179.

55. Gupta R, Bajpai M. Influence of formulation parameters on tizanidine hydrochloride nanoparticles. Int J Pharm Bio Sci. 2013;4(2):1056–1078.

56. Pavithra K, Bhagawati ST, Manjunath K. Development and evaluation of tizanidine hydrochloride loaded solid lipid nanoparticles. Asian J Pharm Clin Res. 2019;12:152–158.

57. Németh Z, Csóka I, Semnani Jazani R, Sipos B, Haspel H, Kozma G, et al. Quality by design-driven zeta potential optimisation study of liposomes with charge imparting membrane additives. Pharmaceutics. 2022;14(9):1798. doi:10.3390/pharmaceutics14091798.

58. Badie H, Abbas H. Novel small self-assembled resveratrol-bearing cubosomes and hexosomes: preparation, characterization, and ex vivo permeation. Drug Dev Ind Pharm. 2018;44(12):2013–2025.

59. Ali Z, Sharma PK, Warsi MH. Fabrication and evaluation of ketorolac loaded cubosome for ocular drug delivery. J Appl Pharm Sci. 2016;6(9):204–208.

60. Boyd BJ, Whittaker DV, Khoo SM, Davey G. Hexosomes formed from glycerate surfactants formulation as a colloidal carrier for irinotecan. Int J Pharm. 2006;318(1-2):154–162.

61. Nath AG, Dubey P, Kumar A, Vaiphei KK, Rosenholm JM, Bansal KK, et al. Recent advances in the use of cubosomes as drug carriers with special emphasis on topical applications. J Lipids.2024;2024:2683466.

62. Mast MP, Modh H, Knoll J, Fecioru E, Wacker MG. An update to dialysis-based drug release testing data analysis and validation using the Pharma Test dispersion releaser. Pharmaceutics. 2021;13(12):2007. doi:10.3390/ pharmaceutics 13122007. PMID: 34959289.

التحضير والتوصيف للناقلات النانوية الكيوبوسومية الحاملة لتزانيدين كنظام توصيل دوائي عبر الجلد

ميلاد جواد حسن*[١،] و نوال عياش رجب[٢]

[١]وزارة الصحة، بغداد، العراق

[٢] فرع الصيدلانيات، كلية الصيدلة ، جامعة بغداد، بغداد ، العراق

الخلاصة

الكيوبوسومات هي مستحلبات نانوية مائية ذات بنية دهنية تتشكل من خلال عملية تجميع ذاتي منظمة وعفوية. يمكن لهذه الأشكال الدوائية المعتمدة على الدهون أن تعمل كحاملات فعالة للأدوية المحبة للدهون والماء، مما يعزز الفعالية العلاجية للأدوية تم تطوير الكيوبوسومات لدراسة فعاليتها كناقلات نانوية لتوصيل تيزانيدين عبر الجلد، وهو مرخي عضلي هيكلي ذو توافر بيولوجي منخفض عند تناوله فمويًا.تم تحضير الحويصلات الكيوبوسومية باستخدام تقنية ترطيب الفيلم الرقيق، حيث تم استخدام جليسيريل مونو أوليات (GMO) كمكون دهني وبولوكسامر ٤٠٧ (P407) كمثبت. وتم تعديل خصائص الحويصلات بتغيير نسبة السطحي إلى الدهون.تم تقييم المستحضرات المحضرة من حيث حجم الحويصلات ، ومؤشر تعدد التشتت ، وكفاءة الاحتجاز .خضعت الصيغة المثلى لمزيد من الدراسات، بما في ذلك دراسة الإطلاق في المختبر، وقياس جهد زيتا، والمجهر الإلكتروني الماسح بالانبعاث الميداني(FESEM) ، وتحليل التوافق باستخدام مطيافية الأشعة تحت الحمراء بتحويل فورييه ، بالإضافة إلى قياس السعرات الحرارية بالمسح التفاضلي لمقارنة الصيغة المثلى بالدواء النقي.أظهرت النتائج تغيرات كبيرة في بعض الخصائص الفيزيائية والكيميائية، مثل حجم الجسيمات وكفاءة الاحتجاز. أظهرت الصيغة المثلى، المسماةF9 ، حجم حويصلات ١٦٠,٧ ± ٤,٧٨٥ نانومتر، ومؤشر تعدد التشتت ٠,٠٦١ ± ٠,٠٤٨، وكفاءة احتجاز ٧٦,٨ ± ٠,١٧٪، وجهد زيتا -٢٣,٤٦ ± ٤,٠٨٨ مللي فولت.كشفت دراسة الإطلاق في المختبر عن نمط إطلاق متحكم ومستدام من الكيوبوسومات. وأكدت الصور الميكروسكوبية أن الحويصلات الكيوبوسومية تمتلك شكلًا مكعبًا موحدًا مع استقرار جيد للتشتت. تشير هذه النتائج إلى أن تقنية ترطيب الفيلم الرقيق تعد طريقة فعالة لتطوير تشتتات كيوبوسومية مستقرة.

الكلمات المفتاحية : كيوبوسومات , تشنج عضلي , تيزانيدين , توصيل عبر الجلد, نظام حويصلي .